RSC Advances

ROYAL SOCIETY OF CHEMISTRY

www.rsc.org/advances

Electron impact scattering by SF_6 molecule over an extensive energy range

Biplab Goswami and Bobby Antony*

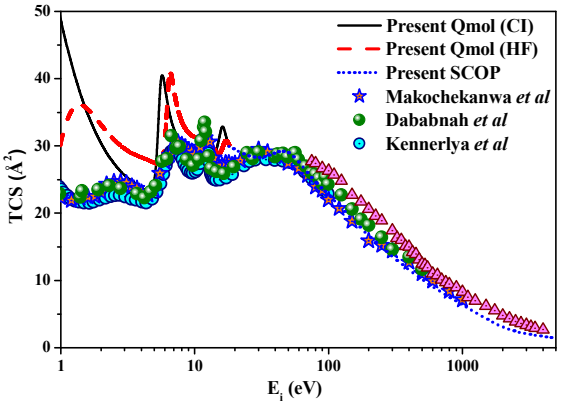

Theoretical elastic and inelastic cross sections for e-SF_6 scattering over 0.1-5000 eV energies are reported employing R-matrix and SCOP formalisms.

Cite this: DOI: 10.1039/c0xx00000x

www.rsc.org/xxxxxx

PAPER

Electron impact scattering by SF_6 molecule over an extensive energy range

Biplab Goswami and Bobby Antony*

Received (in XXX, XXX) Xth XXXXXXXXX 20XX, Accepted Xth XXXXXXXXX 20XX
DOI: 10.1039/b000000x

The present article reports the theoretical total cross sections for e-SF_6 scattering over the energy range 0.1-5000 eV. For low energy calculations upto ionization threshold of the target the *ab-initio* R-matrix formalism is employed and beyond that energy spherical complex optical potential method is used. Elastic, electronic excitation, rotational excitation, momentum transfer and total cross sections were calculated and presented for the low energy calculations. Differential elastic cross sections for various energies are also reported here. We have identified and detected two resonances at 5.43 and 17.02 eV energies with the possibility of anions formations. The present results show reasonable accord with the existing theoretical and experimental results, wherever available. The rotational excitation cross sections reported for e-SF_6 scattering system is a first attempt.

I. Introduction

Sulphur hexafluoride (SF_6) molecule is one of the very important fluorine containing feed gas[1] presently being utilized. This molecule is used suitably in semiconducting industry for dry plasma etching in material processing[2]. The insulating properties of this molecule make it demanding in the electric power technology particularly as gaseous dielectric material[3]. However, SF_6 is a potent green house gas with a global warming potential 23,900 times as strong as CO_2 and a 3,200-year residence lifetime in the environment[4]. SF_6 is also an efficacious infrared absorber and hence plays a key role in the atmospheric photochemistry as ozone depleting molecule[5]. This molecule is used appreciably in magnesium and aluminium industry as a heavier and inert cover gas to isolate the molten magnesium from oxygen and to reduce the porosity of cast aluminium, particularly in casting operation[6]. SF_6 is highly acceptable as a 'self healing' dielectric to the interrupting medium, since dielectric strength of this gas is satisfactorily stable in the decomposition process[7]. Hence, the necessity of various electron collision cross sections for SF_6 over a wide energy domain are indispensable, particularly to study the physio-chemical processes in electron rich gaseous medium.

In recent years, various investigation of electron impact scattering by SF_6 molecules were reported both theoretically and experimentally by different groups owing to the environmental issues and for its enormous application in industry as discussed earlier. Makochekanwa *et al.*[8], Dababneh[9], Kennerlya *et al.*[10], Kasperski *et al.*[11], Zecca *et al.*[12], Wan *et al.*[13], Ferch *et al.*[14], Trajmar *et al.*[15], Limão-Vieira *et al.*[16] and Rohr[17] measured electron impact total cross sections for SF_6, while Cho *et al.*[18], Srivastava *et al.*[19], Johnstone and Newell[20] and Sakae *et al.*[21] reported the experimental differential and integral elastic cross sections. Benedict and Gyemant[22] calculated electron impact total elastic cross sections using a multiple scattering method. The momentum transfer cross sections were obtained by Phelps and Van Brunt[23] and Christophorou and Olthoff[24]. Winstead and McKoy[25] calculated differential, elastic and momentum transfer cross sections for electron scattering with SF_6 molecule using Schwinger Multichannel (SMC) method in the energy range 0.5-75 eV, while Dehmer *et al.*[26] reported theoretical cross section results between 0-40 eV impact energies for elastic collision. Limão-Vieira *et al.*[16] calculated total cross section for 100-10000 eV energy range using independent atom model approximation and a modified single-center additivity rule. Calculations for differential, elastic, momentum transfer cross section have also been performed by Gianturco *et al.*[27], Gianturco and Lucchese [28], Jiang *et al.*[29], Johnstone and Newell[30] applying different theoretical formalisms. Shi *et al.*[31] and M. Vinodkumar *et al.*[32] calculated total cross sections between 30-5000 eV and 15-2000 eV for electron scattering with SF_6 molecule using Modified additivity rule and Modified Single Centre-Additivity Rule (MSC-AR) rule respectively. From 10-2000 eV energies Joshipura *et al.*[33] used spherical complex optical potential (SCOP) formalism to calculate total cross section for e-SF_6 scattering. Fabrikant *et al.*[34] calculated integral elastic, differential cross sections between 0.2-5 eV energies using Effective range theory. A summary of literature survey for electron scattering with SF_6 is given in Table 1.

From the table 1, it is clear that there is a whole lot of interest in the electron impact cross section of SF_6 molecule. The total cross section (TCS) studies are comprehensive in terms of both theoretical and experimental endeavours. However, there are no previous results reported for electronic excitation or rotational excitation cross sections. Also, the differential cross section (DCS), momentum transfer cross section (MTCS) reported are fragmentary. Besides, most of the previous studies are confined to a small energy range. Different cross section data for various scattering channels covering a wider energy domain are still lacking.

Cite this: DOI: 10.1039/c0xx00000x

www.rsc.org/xxxxxx

PAPER

Table 1 Review of literature for e-SF_6 scattering.

Energy Range (eV)	Cross section	Reference	Method (Exp-Experimental; Th-Theoretical)
1-500	TCS	Dababneh[9]	Beam Transmission technique (Exp)
0.5-75	Elastic, DCS, MTCS	Winstead and McKoy[25]	SMC (Th)
0-40	Elastic	Dehmer *et al.*[26]	Multichannel model (Th)
0.5-100	TCS	Kennerlya *et al.*[10]	Time of flight analysis (Exp)
0.8-100	TCS	Makochekanwa *et al.*[8]	Linear Transmission type Time of flight Instrument (Exp)
0.036-1	TCS	Ferch *et al.*[14]	Time of fight mass spectrometry (Exp)
0.03-1	TCS	Trajmar *et al.*[15]	Time of flight technique (Exp)
2.7-75	Elastic, DCS	Cho *et al.*[18]	Crossed electron-molecular beam spectrometer (Exp)
100-10000	TCS	Limão-Vieira *et al.*[16]	Transmission beam system (Exp) Independent atom model approximation and a modified single-center additivity rule (Th)
meV-100 eV	Elastic, DCS, MTCS	Gianturco and Lucchese[28]	*ab-initio* static exchange correlation polarization (SECP) potential approach (Th)
100-700	Elastic, DCS, MTCS	Jiang *et al.*[29]	Independent atom model with partial waves (Th)
75-700	Elastic, DCS, MTCS	Sakae *et al.*[21]	Crossed beam method (Exp)
75-4000	TCS	Zecca *et al.*[12]	Ramsauer-type electron spectrometer (Exp)
30-5000	TCS	Shi *et al.*[31]	Modified additivity rule (Th)
15-2000	TCS	M. Vinodkumar *et al.*[32]	MSC-AR (Th)
10-2000	TCS, Ionization, Excitation	Joshipura *et al.*[33]	SCOP formalism (Th)
0.2-5	Integral, DCS	Fabrikant *et al.*[34]	Effective range theory (Th)
0-30	Elastic, DCS	Gianturco *et al.*[27]	*ab-initio* exact static exchange plus polarization (SEP) approach with Close-Coupling (CC) formulation (Th)
5-75	Elastic, DCS, MTCS	Johnstone and Newell[30]	Hemispherical electron spectrometer (Exp)
0.3-10	Integral, DCS	K Rohr[17]	Crossed-beam technique (Exp)
0-12	TCS	Wan *et al.*[13]	Electron transmission spectrometer (Exp)
10-60	Elastic	Benedict and Gyemant[22]	Multiple scattering method (Th)

In this article we report total cross section for e-SF_6 scattering from 0.1-5000 eV impact energies. The differential, electronic excitation and rotational excitation cross sections are also calculated for low energies. Resonances are also located at two different energies with the possibilities of anion formation.

The organization of the paper is as follows: section II explains the theoretical methodologies employed in the present calculations, section III describes the results obtained and discussions of the present study and finally section IV summarizes and concludes this work.

II. Theoretical Methodology

In this article electron impact cross sections with SF_6 molecule are reported. For this purpose two formalisms were employed: *ab initio* R-matrix[35] calculations using Quantemol-N[36] module for low energies and SCOP[37-40] formalism for intermediate to high energies. These methods are separately explained in the following subsections. However, before that the target model employed for the low energy calculations are depicted here.

A. Target model.

SF_6 is an octahedral molecule with S-F bond length of 1.561Å[2 41]. A 6-31G Gaussian basis set is employed for the representation of target wave function, since the wave function of the system becomes converged upto ionization threshold of the target by using the current basis set. SF_6 molecule is considered to be in the D_{2h} point group (subgroup of O_h point group) for the present low energy calculations. The ground-state Hartree-Fock electronic configuration for the SF_6 molecule is represented as $1A_g^2$, $2A_g^2$, $1B_{2u}^2$, $1B_{3u}^2$, $1B_{1u}^2$, $1B_{1g}^2$, $3A_g^2$, $4A_g^2$, $2B_{3u}^2$, $2B_{2u}^2$, $2B_{1u}^2$, $5A_g^2$, $3B_{3u}^2$, $3B_{2u}^2$, $3B_{1u}^2$, $2B_{1g}^2$, $6A_g^2$, $7A_g^2$, $4B_{2u}^2$, $4B_{3u}^2$, $4B_{1u}^2$, $8A_g^2$, $1B_{2g}^2$, $1B_{3g}^2$, $1A_u^2$, $5B_{3u}^2$, $5B_{2u}^2$, $6B_{3u}^2$, $6B_{2u}^2$, $5B_{1u}^2$, $3B_{1g}^2$, $2B_{2g}^2$, $2B_{3g}^2$, $4B_{1g}^2$, $9A_g^2$. Out of the 70 electrons we have frozen 66

electrons in the $1A_g$, $2A_g$, $3A_g$, $4A_g$, $5A_g$, $6A_g$, $7A_g$, $8A_g$, $1B_{3u}$, $2B_{3u}$, $3B_{3u}$, $4B_{3u}$, $5B_{3u}$, $6B_{3u}$, $1B_{2u}$, $2B_{2u}$, $3B_{2u}$, $4B_{2u}$, $5B_{2u}$, $6B_{2u}$, $1B_{1g}$, $2B_{1g}$, $3B_{1g}$, $1B_{1u}$, $2B_{1u}$, $3B_{1u}$, $4B_{1u}$, $5B_{1u}$, $1B_{2g}$, $2B_{2g}$, $1B_{3g}$, $2B_{3g}$, $1A_u$ molecular orbitals, while the remaining 4 electrons allowed to move freely in active space of $9A_g$, $10A_g$, $11A_g$, $12A_g$, $7B_{3u}$, $8B_{3u}$, $7B_{2u}$, $8B_{2u}$, $4B_{1g}$, $6B_{1u}$, $7B_{1u}$, $3B_{2g}$, $3B_{3g}$ orbitals. A total number of 349 configuration state functions (CSFs) are considered in the close coupling expansion for the representation of seventeen target states.

For the static exchange plus polarization (SEP) calculations with this *ab-initio* R-matrix method, first of all we generate target properties by constructing the transition density matrix utilizing GAUSPROP and DENPROP[42] modules of the UK R-matrix software suite. The multipole transition moments in inner region calculations were obtained using the second-order perturbation theory and the property integrals computed by GAUSPROP[42].

The present SEP calculation resulted in ground state energy of -993.5344 hartree for the SF_6 molecule which is in good accord with the theoretical value -993.786672 hartree[28]. The present rotational constant of 0.09102 cm^{-1} matches very well with the experimental value of 0.09107 cm^{-1} [43] and the calculated value of 0.090686 cm^{-1} [44]. The computed dipole moment for SF_6 is zero which agrees with the previously measured dipole moment[45]. The first electronic excitation energy for SF_6 is found to be 11.5942 eV showing good agreement with the calculated value 11.19[25]. These target properties along with the available comparison are given in Table 2.

Table 2 Target properties obtained in the present calculation along available comparison.

Properties of SF_6	Present	Experimental	Theoretical
Ground-state energy (hartree)	-993.5344	-	-993.786672[28]
First excitation energy (eV)	11.5942	-	11.19[25]
Rotational constant (cm^{-1})	0.09102	0.09107[43]	0.090686[44]
Dipole moment (D)	0	0[45]	-

B. Low energy formalism (1 eV ~ 18 eV)

The *ab-initio* R-matrix method is one of the most useful formalism for low energy calculations. The low energy scattering problem can also be represented by Green's function which is a useful tool in mathematical physics. For the representation of electron scattering in a general scattering geometry Wong[46] introduced the properties and solution of the Green's functions. Recently, Altunata *et al.*[47] have applied an *ab-initio* R-matrix method using an iterative Green's-function for calculating the molecular reaction matrix of scattering theory with smooth energy dependence. This method mostly takes care of all the polarization effects and considers both polar and nonpolar ion cores in a unified fashion and is equally valid for both short and long range potentials. The closed-form analytic expressions for one and two-electron integrals of Cartesian Gaussian orbitals outside the R-matrix sphere is given by Wong *et al.*[48] which can be used in *ab-initio* molecular scattering calculations. It is a known fact that R-matrix method is the most widely used *ab-initio* methods. In the present wok we have employed R-matrix method through Quantemol-N[36] package. The fundamental concept behind R-matrix formalism is based on the division of configuration space into two specified regions, namely inner and outer region. The inner region is chosen such that it fits all the target wave functions of the molecule. For the present molecule we have taken inner region radius as $13a_0$. This value is chosen such a way that the result becomes convergent. All of the N+1 electrons are confined to this region, which makes the inner region calculations complex, but definite. In this region various short range potentials viz. static, exchange, absorption and electron-electron correlation polarization become influential as the wave functions are compact in inner region problem. Whereas in outer region, exchange and correlation potential are assumed to be negligible and only long-range multipolar interactions between target and scattering electrons become dominant. For simple and fast computations, the outer region problem is approximated as a single-centre and for the present calculations the outer region radius is expanded up to 100 a_0.

The wave function for the system using close-coupling approximation[49] for the inner region problem can be specified as,

$$\psi_k^{N+1} = A\sum_I \psi_I^N(x_1,\cdots;x_N)\sum_j \zeta_j(x_{N+1})a_{Ijk} + \sum_m \chi_m(x_1,\cdots;x_{N+1})b_{mk} \quad (1)$$

Where A is the anti-symmetrization operator imposed on electrons in the inner region to obey the Pauli principle, x_N is the spatial and spin coordinate of the N^{th} electron, Φ_i^N is the i^{th} state of the N-electron target which is represented using a configuration integration (CI) expansion and ξ_j is the continuum orbital spin coupled with the target states. The coefficients a_{ijk} and b_{mk} are variational parameters. The second summation in equation (1) contains functions χ_m which describes all the N +1 electrons as L^2 configurations that disappear at $r = a$. They are included to relax the scattering and target orbitals of the equal symmetry in the molecule. The single excited L^2 term incorporates the polarization effect to the Hartee-Fock (HF) ground state wave function. This scattering model is denoted as static exchange plus polarization model. Here lowest numbers of target states are used for the close-coupled calculations. This is included to account for the orthogonality relaxation and short-range polarization effects by a CI expansion in the first summation and over a hundred configurations in the second.

For the molecular electronic-structure calculations, the target wave functions are represented by basis-function expansion. There Gaussian-type orbitals (GTOs) and the continuum orbitals of Faure *et al.*[50] are utilized in that quantum-chemical package. The advantage of GTOs is that the multi-centred integral can be treated analytically to achieve fairly improved accuracy in the calculations. The inner region calculation is propagated to the outer region potential, until its solutions agree with the

asymptotic functions given by the Gailitis expansion[51]. Hence, the R-matrix maintains a bridge between the inner and outer region. In the outer region problem the coupled single centre equations are integrated to deduce all the observable by employing K-matrices. The K-matrices are employed to obtain T-matrices using the definition

$$T = \frac{2iK}{1 - iK} \quad (2)$$

The T matrices are then used to calculate the cross sections in the outer region. To identify the position and width of the resonances, eigenphase sum is fitted with Breit-Wigner form[52]. The differential cross section calculations are performed by processing of K matrices through the approach reported by Sanna and Gianturco[53].

C. High energy formalism.

The elastic and inelastic processes play crucial roles in electron-molecule interaction systems at high impact energies too. In the present work the high energy calculations are performed by spherical complex optical potential (SCOP) formalism[37-40]. In SCOP method, a complex potential is constructed and used to solve Schrödinger equation. The potential may be expressed as:

$$V_{opt}(r, E_i) = V_R(r) + iV_I(r, E_i) \quad (3)$$

Where the real part is given by,

$$V_R(r, E_i) = V_{st}(r) + V_{ex}(r, E_i) + V_p(r, E_i) \quad (4)$$

The static potential $V_{st}(r)$ is a function of radial vector (r) only, whereas exchange and polarization potentials depends on both r and incident energy of the particle (E_i). Utilizing the unperturbed Hartree-Fock wave function we can calculate the static potential, $V_{st}(r)$. The short range correlation and the long range polarization effect is expressed by $V_p(r,E_i)$ and the electron exchange interaction is given through $V_{ex}(r,E_i)$. All these potentials given in equation (4) depend on the electronic charge density of the molecule. The parameterized Hartree-Fock wavefunctions given by Salvat *et al.*[54] is applied here to find the radial electron charge density of the molecule.

The exchange potential, V_{ex} is formulated using the 'Hara free-electron gas exchange' model[55] and polarization potential, V_p using the parameter free model of correlation-polarization potential given by Zhang *et al.*[56]. For consistent results in the intermediate region Zhang *et al.*[56] have incorporated various non-adiabatic corrections that will approach the correct asymptotic form at large 'r'. The two non-spherical terms, vibrational and rotational excitations of the target, are not included for high energy calculations in our model potential. This is justified because the time of interactions of the incident electron with the target in the intermediate to high energy range is sufficiently small compared to the vibrational and rotational times, and hence the cross section due to these processes are negligible.

The absorption potential, V_{abs} accounts for the total loss of flux due to excitation and ionization through these scattering channels. To represent this we have used a model potential given by Staszewska *et al.*[57]. This absorption term is represented as,

$$V_{abs}(r, E_i) = -\rho(r)\sqrt{\frac{T_{loc}}{2}}\left(\frac{8\pi}{10k_F^3 E_i}\right)\theta(p^2 - k_F^2 - 2\Delta)(A_1 + A_2 + A_3) \quad (5)$$

Where the local kinetic energy of the incident electron is

$$T_{loc} = E_i - (V_{st} + V_{ex} + V_p) \quad (6)$$

In equation (5), $p^2 = 2E_i$, $k_F = [3\pi^2 \rho(r)]^{1/3}$ is the Fermi wave vector and A_1, A_2 *and* A_3 are dynamic functions that depends differently on $\theta(x)$, I, Δ and E_i. I is the ionization threshold of the target, $\theta(x)$ is the Heaviside unit step-function and Δ is an energy parameter below which $V_{abs} = 0$. So Δ is an important factor that determines the values of total inelastic cross section and below this energy the ionization or excitation is not allowed. This is one of the notable features of Staszewska model[57]. However, fixing $\Delta = I$ will restrict all the inelastic processes with threshold lower than ionization potential. This is a serious drawback of the theory and to fix this we have considered Δ as a slowly varying function of E_i around I. Also, if Δ is much smaller than the ionization threshold, then V_{abs} becomes unexpectedly high near the peak position. So we have introduced a minimum value of 0.8 I to Δ and varied it as a function of E_i around I by the following formula:

$$\Delta(E_i) = 0.8I + \beta(E_i - I) \quad (7)$$

The parameter β is determined by considering that $\Delta = I$(eV) at $E_i = E_p$, the value of incident energy at which present Q_{inel} becomes maximum. E_p can be found by calculating Q_{inel} by keeping $\Delta = I$. Beyond E_p, Δ is kept as I. The expression given in eqn (7) is meaningful as it would allow electronic excitations below ionization potential as well.

The radial Schrödinger equation is solved by using the full complex optical potential, given in Eqn. (3). The solutions of the asymptotic scattering equation are obtained in the form of complex phase shifts (δ_l) for each partial wave. The phase shifts carries all the necessary information regarding the scattering event. The knowledge of the phase shift is utilized to compute the scattering amplitude as,

$$f(k,\theta) = \frac{1}{2ik}\sum_{l=0}^{\infty}(2l+1)[S_l(k) - 1]P_l(\cos\theta) \quad (8)$$

Where $S_l(k) = \exp(2i\delta_l)$ is called S-matrix (scattering matrix) elements constructed using δ_l. Hence equation (8) can be written as,

$$f(k,\theta) = \frac{1}{2k}\sum_{l=0}^{\infty}(2l+1)\exp(i\delta_l)\sin\delta_l P_l(\cos\theta) \quad (9)$$

Thus the total inelastic cross section, Q_{inel} and total elastic cross section, Q_{el} can be calculated employing scattering amplitude as above through standard relations[58],

$$Q_{inel}(E_i) = \frac{\pi}{k^2}\sum_{l=0}^{\infty}(2l+1)(1-\eta_l^2) \quad (10)$$

and

$$Q_{el}(E_i) = \frac{\pi}{k^2}\sum_{l=0}^{\infty}(2l+1)\left|\eta_l \exp(2i\,\mathrm{Re}\,\delta_l)-1\right|^2 \quad (11)$$

where $\eta_l = \exp\left(-2\,\mathrm{Im}\,\delta_l\right)$ is called the inelasticity or absorption factor for each partial wave. Then the total cross section, Q_T will be the sum of these two cross sections.

III. Results and Discussions

In this article, a comprehensive computational study of electron collision with SF_6 in gas phase is reported. The primary aim of this work is two-fold: (1) to detect the position of resonances, if any, by studying the eigenphase diagram and (2) to present elastic and total cross sections for an extensive energy domain (0.1-5000 eV). Besides, we have also reported elastic DCS, electronic excitation cross section, MTCS and rotational excitation cross sections. The *ab-initio* R-matrix method is used at low energies through Quantemol-N[36] module, as it gives reliable results up to the ionization threshold of the target. For high energy calculations the spherical complex optical potential (SCOP) formalism[37-40] is used. The Q_T obtained from these two theories matches smoothly at the overlap energy (~18 eV) and thus allowing us to predict total cross sections for this wide energy range.

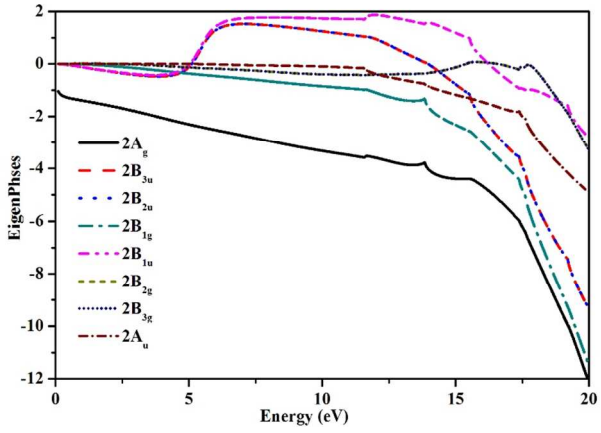

Fig. 1 Eigenphase diagram for e-SF_6 scattering.

The eigenphase diagram of various doublet states ($2A_g$, $2B_{3u}$, $2B_{2u}$, $2B_{1g}$, $2B_{1u}$, $2B_{2g}$, $2B_{3g}$, $2A_u$) for the e-SF_6 system is potted in figure 1. The eigenphase diagram shows shape resonances at 5.43 eV belonging to the T_{1u} symmetry of the O_h group, which splits into the $2B_{1u}$, $2B_{2u}$, and $2B_{3u}$ symmetries of the D_{2h} group. The present resonance appears towards the lower energy compare to the resonance at 7 eV reported by the measurement of Dababneh[9] and Kennerlya *et al.*[10] and calculations of Fabrikant *et al.*[34] as given in table 3. The resonance at 5.43 eV is confirmed by a sharp peak in total cross section (see figure 3) at the same energy. Another sharp feature is seen at around 17 eV due to $2A_u$ state, contributing significantly to the hump appearing in the total cross section around that energy.

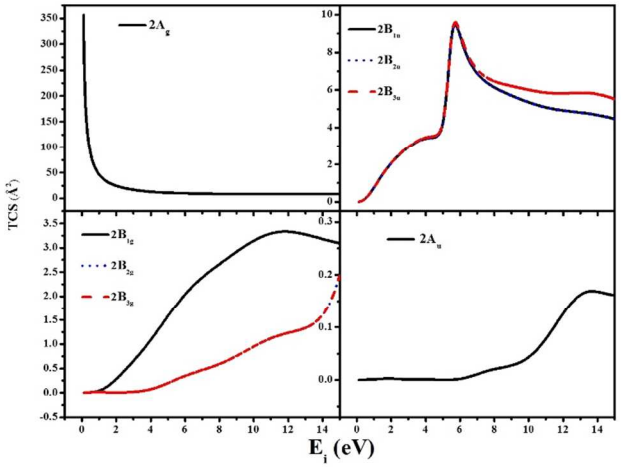

Fig. 2 Symmetry components of the total cross section for electron scattering by SF_6

The contribution of various symmetries to the total cross section in SEP calculations for SF_6 has been presented in figure 2. It is quite obvious that the contributions are quite different for different symmetries. At low impact energy studied here, the collisions tend to dominate here by the contribution of s-wave channel. The intense high cross section at low energies is due to the s-wave ($2A_g$ symmetry) as shown in figure 2. From the above figure, it is clear that the shape resonances appearing at about 5.43 eV is mainly due to the contribution from $2B_{1u}$, $2B_{2u}$ and $2B_{3u}$ symmetries.

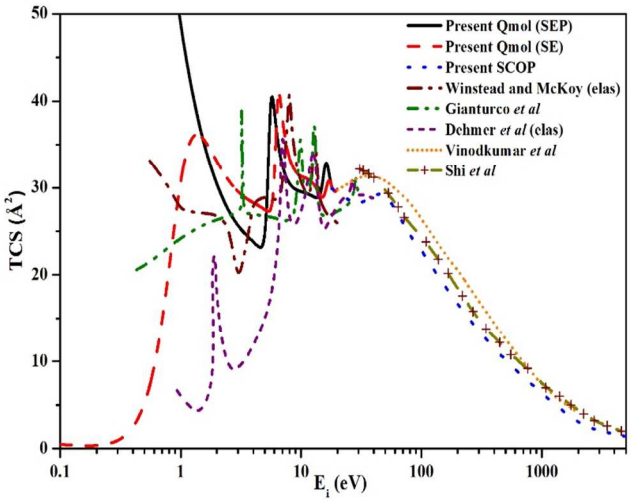

Fig. 3(a) Total cross section for e-SF_6 scattering with theoretical comparisons. Solid line: Present Qmol (SEP), dashed line: Present Qmol (SE), dotted line: Present SCOP, dash dotted line: Winstead and McKoy (elas)[25], dash-dot dotted line: Gianturco *et al.*[27], short dashed line: Dehmer *et al.* (elas)[26], short dotted line: Vinodkumar *et al.*[32], dash-plus line: Shi *et al.*[31]

In fig. 3(a) and fig. 3(b) we present total cross sections from 0.1-5000 eV impact energies with the available theories and experiments respectively. To display the resonance peaks clearly, we have cut the y-axis in both figures at 50 Å^2. The results shown in fig.3(a) gives reasonably good agreement with previous theoretical studies. At very low energies (<1 eV), present SE calculations displays a peak at 1.36 eV matching quite well with the position of peak by Dehmer *et al.*[26], while the total cross sections for present SEP calculations shows asymptotic behaviour. The present SEP calculation depicts sharp peaks at 5.4 eV of about 17 Å^2 due to the contribution of shape resonances from $2B_{1u,}$ $2B_{2u}$ and $2B_{3u}$ states. The peak is found to be shifted slightly to higher energy side (6.54 eV) for the SE calculations. The rise in TCS for elastic cross sections of Winstead and McKoy[25] is at 7.98 eV. A sharp peak is also reported by Gianturco *et al.*[27] which is at much lower energy than these data. The elastic cross section reported by Dehmer *et al.*[26] also shows similar structure, but with much lower magnitude. The data by Vinodkumar *et al.*[32] shows similar shape and magnitude throughout the energy range. Shi *et al.*[31] have used a modified additivity rule to report the total cross section and it falls very close to our data. The interesting fact here is that present data by R-matrix method and SCOP method shows consistency at about 20 eV. This convergence has helped us to predict cross section from 0.1 eV to 5000 eV.

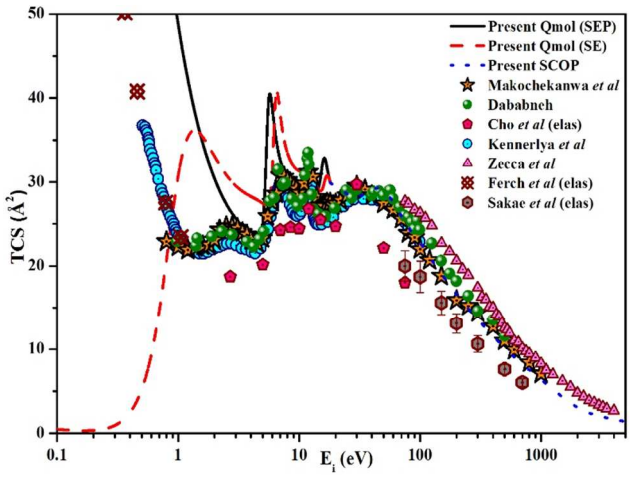

Fig. 3(b) Total cross section for e-SF_6 scattering with experimental comparisons. Solid line: Present Qmol (SEP), dashed line: Present Qmol (SE), dotted line: Present SCOP, star: Makochekanwa *et al.*[8], solid circle: Dababneh[9], solid pentagon: Cho *et al.*[18], solid circle-dot: Kennerlya *et al.*[10], solid triangle: Zecca *et al.*[12], rumbas-cross: Ferch *et al.*[14], hexagon-dot: Sakae *et al.* (elas)[21].

In fig 3(b) we can see that below 1 eV the present SEP results are much higher than the SE results. However, the shape of the SEP data shows similar nature as that of the measurements by Kennerlya *et al.*[10] and Ferch *et al.*[14]. The present peak shows a reasonable agreement with that of the experiments by Kennerlya *et al.*[10] (7 eV), Dababneh[9] (6.7 eV) and Cho *et al.*[18] (8.5 eV). However, the magnitude of cross section is quite lower for the measurements. Another maximum is seen at 16.14 eV for the present SEP calculations which is due to the excited states $1A_g$ and $1B_{1g}$ at that energy. The measurements also report a secondary peak, even though they do not fall at the same energy. After 20 eV the present results merge nicely with the measurements of Dababneh[9] and Kennerlya *et al.*[10]. The measurements reported by Zecca *et al.*[12] are higher than all other data presented here. In general, the inclination manifested by our theoretical data is very much in congruence with previous experimental results. The present total cross sections data from 0.1-5000 eV is presented in table 3.

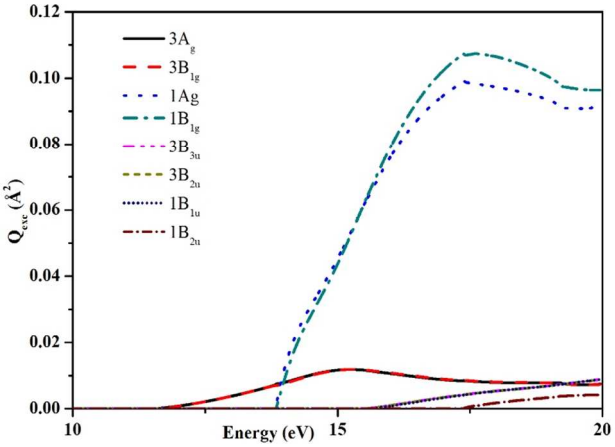

Fig. 4 Electronic excitation cross sections for e-SF_6 scattering.

The electronic excitation cross sections from the ground state $1A_g$ to eight low lying excited states $3A_g$, $3B_{1g}$, 1Ag, $1B_{1g}$, $3B_{3u,}$ $3B_{2u,}$ $1B_{1u}$ and $1B_{2u}$ are shown in figure 4. The threshold of vertical excitation energies for both triplet states $3A_g$ and $3B_{1g}$ are 11.594 eV and 11.597 eV respectively showing agreement with the first electronic transition at 11.19 eV of Winstead and McKoy[25]. However, present calculation of first excitation energy displays good agreement with the first strong continuum reported at 11.6 eV in the absorption spectrum of Trajmar and Chutjian[59]. There is also a prominent feature at around 17 eV in the excitation curves for $1A_g$ which coincides with the resonance due to $1B_{1g}$ reported earlier.

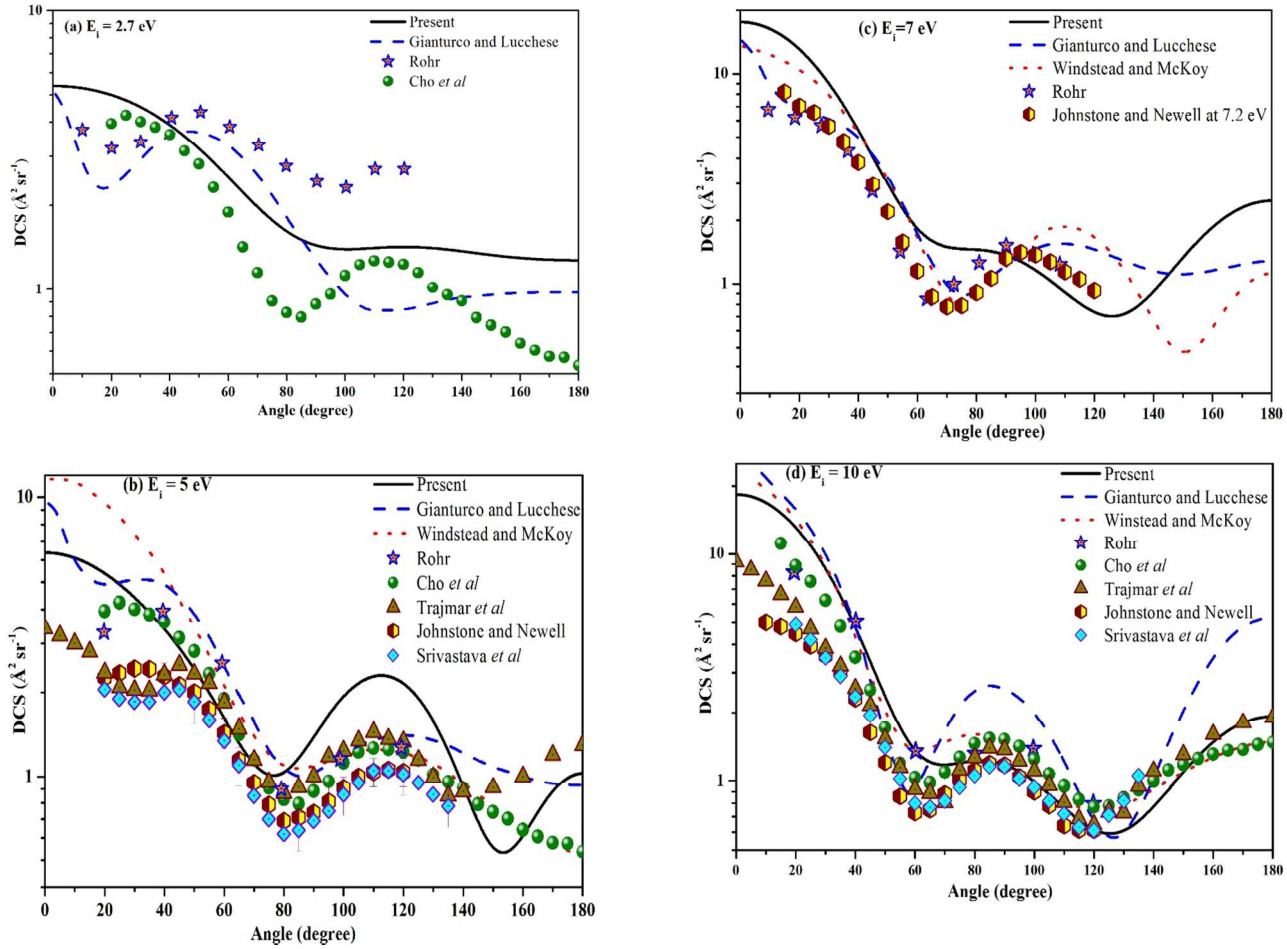

Fig. 5(a-d) Differential cross section for e-SF_6 scattering system from 2.7 eV-10 eV. Solid line: Present, dashed line: Gianturco and Lucchese[28], dotted line: Winstead and McKoy[25], stars: Rohr[17], circles: Cho *et al.*[18], triangles: Trajmar *et al.*[15], hexagons: Johnstone and Newell[20], rhombuses: Srivastava *et al.*[19].

The differential cross sections are very sensitive to the use of different scattering formalisms and can be accurately measured by experiments and hence leads fair test of any scattering theories. This has prompted us to calculate and present differential cross sections of elastic scattering by electrons for SF_6 molecule particularly from energies 1-10 eV. For comparison, we report only those energies where previous data are available and are given in figures 5(a)-5(d). From figure 5(a) the DCS for 2.7 eV impact energy shows similar shape with the experiment of Rohr[17] and Cho *et al.*[18]. However, all the data are not consistent with each other. At 5,7,10 eV the DCS matches quite well with the calculation of Winstead and McKoy[25] and experiment of Rohr[17] and Trajmar *et al.*[15]. The humps in the DCS are shifted backward for higher impact energies and follow the similar trend of the measurements by Rohr[17] and Cho *et al.*[18] for most of the energies.

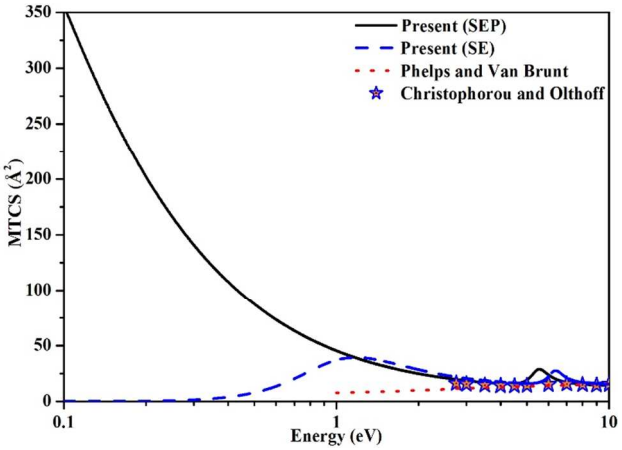

Fig. 6 Momentum transfer cross sections for e$^-$-SF_6 scattering system.

The momentum transfer cross sections (MTCS) for electron collision with SF_6 are shown in figure 6. MTCS is an important ingredient in the plasma modelling. The MTCS reported by Phelps and Van Brunt[23] seems to diverge from present results and that of Christophorou and Olthoff[24] towards the low energy region. The measurements of Christophorou and Olthoff[24] shows a similar trend as that of present results, except the sharp rise around 5-6 eV. The appearance of the sharp peak is due to the resonance at about that energy, which is missing in both previous results.

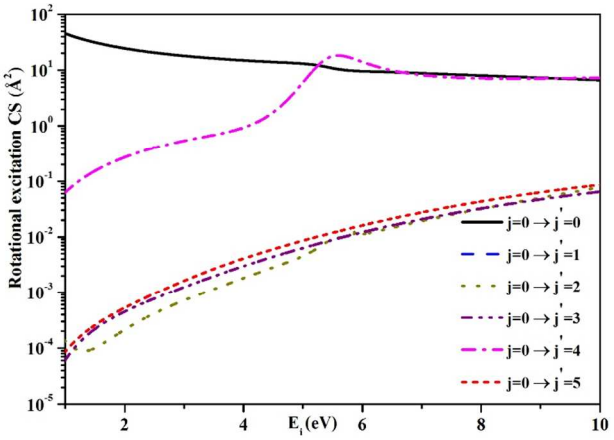

Fig. 7 Rotational excitation cross sections for e-SF_6 scattering system.

In Fig. 7 we have plotted the electron impact rotational excitation cross sections for SF_6 molecule. The maximum contribution in total rotational excitation cross sections comes from the j=0→j'=0 state. At low energy the rotational cross section for j=0→j'=0 state becomes considerably high due to the long range effect. The 16-pole moment of SF_6 gives very high long range force to the scattering electron, hence the target feel the torque even when the incident electron is further away from the target, and so more time to impart a rotational force on the molecule. It is noticeable that the doublet and quartet rotational excitations (j=0→j'=4 and j=0→j'=2) matches quantitatively, whereas the triplet and quintet excitations (j=0→j'=3 and j=0→j'=5) also depict similar features. For the j=0→j'=4 and j=0→j'=2 states a hump is observed at about 5.5 eV, which is near to the position of shape resonance at 5.43 eV.

Table 3 TCS for e-SF_6 scattering.

Energy (eV)	TCS (Å^2) (QMOL)	Energy (eV)	TCS (Å^2) (SCOP)
0.1	356.69	18	29.89
0.2	203.71	20	29.47
0.3	142.65	22	29.03
0.5	89.74	24	28.71
1.0	48.80	26	28.44
1.5	36.08	28	28.32
2.0	30.40	30	28.27
2.5	27.38	32	28.33
3.0	25.64	34	28.47
3.5	24.57	36	28.64
4.0	23.79	38	28.86
4.5	23.19	40	28.99
5.0	24.92	42	29.17
5.2	28.73	44	29.25
5.5	37.94	46	29.26
5.7	40.48	48	29.19
5.8	40.31	50	29.06
6.0	38.77	60	27.60
6.5	34.82	70	25.95
7.0	32.55	80	24.62
8.0	30.51	90	23.57
9.0	29.81	100	22.80
10	29.55	200	16.33
12	29.13	500	9.91
15	30.47	1000	6.37
16	32.81	2000	2.78
17	31.74	5000	1.40

IV. Conclusion

A comprehensive work to calculate differential elastic, total elastic, electronic excitation, rotational excitation, momentum transfer and total cross section for electron collision with SF_6 molecule has been performed and reported in this article. The target properties obtained from close coupling calculations with 6-31G Gaussian basis set and considering the molecule in D_{2h} point group shows reasonable agreement with the available experimental and theoretical results. Hence, the target representation is considered to be justified. The position and width of resonances for low energies are detected using the eigenphase diagram. From figure 1, we can see noticeable features for the $2B_{1u}$, $2B_{2u}$ and $2B_{3u}$ symmetries at 5.43 eV confirming the presence of shape resonance around that energy. The eigenphase presented here tend to go $\pi/2$ instead of zero at low impact energies. At 17.02 eV a short pulsed resonance is also found to appear for the $2B_{1g}$ symmetry. The low energy cross sections become sufficiently high due to the contributions s-wave ($2A_{1g}$ symmetry). The reason to get high elastic cross section at low energy is due to large positive s-wave scattering length of SF_6 molecule. This signifies that the well known virtual state effect can't occur in SF_6 like that observed for C_6F_6 molecule by the calculations of Field *et al.*[60]. Furthermore, for the virtual state scattering at low energy the s-wave phase shift should be high and negative and hence the behaviour of elastic cross section for $2A_{1g}$ symmetry is very much higher (figure 2) as the s-wave scattering length of SF_6 is positive at low energies[60]. The total cross section for different symmetries also reflects a clear enhancement of cross section at these resonant energies as shown in figure 2. The results presented here shows reasonable good agreement quantitatively and qualitatively with the available previous theories and experiments. The present DCS also shows very good match with the existing results.

As discussed earlier there are many previous attempts to study electron induced chemistry with SF_6 molecule due to its importance in various applications. However, the results are

fragmentary and inconsistent as they were independent studies with varying degrees of approximations and difference in experimental set up. A complete study under a common umbrella was lacking. Hence, we have undertaken this task for calculating various cross sections under a hybrid methodology (R-Matrix + SCOP) which can deliver the cross sections for a wide energy range (0.1-5000 eV). This would of great significance to various applications, particularly for the modelling of industrial plasma and the atmospheric research.

Acknowledgements

Authors would like to acknowledge W. J. Brigg, Department of Physics and Astronomy, University College London, UK for helpful discussions at the early stage of the calculations. BA is pleased to acknowledge the support of this research by the Department of Science and Technology (DST), New Delhi through Grant No. SR/S2/LOP-11/2013.

Notes and references

Department of Applied Physics, Indian School of Mines, Dhanbad, 826004, Jharkhand, India. Tel: +91 9470194795; E-mail: bka.ism@gmail.com

1. L. G. Christophorou, J. K. Olthoff and D. S. Green, *"Gases for Electrical Insulation and Arc Interruption: Possible Present and Future Alternatives to Pure SF_6"* National Institute of Standards and Technology (NIST), NIST Technical Note, 1997, 1425.
2. For example, see, *Plasma Processing of Materials* (National Academic Press, Washington, DC, 1991.
3. N. G. Trinh and N. Cuk, *"Practical Considerations for Industrial Applications of SF_6 / N_2 Mixtures,"* Canadian Electrical Association Engineering and Operating Div. Trans., 1984, Vol. **23**, Pt.1, 84-A-60, Canadian Electrical Association, Montreal.
4. IPCC. *Climate Change 2001: A Scientific Basis.* Cambridge University Press, Cambridge, UK, 2001.
5. J. Gajević, M. Stević, J. Nikolić, M. Rabasović and D. Markushev, *Physics, Chemistry and Technology,* 2006, **4**, 57.
6. S. L. Couling, F. C. Bennett and T. E. Leontis, *Melting Magnesium Under Air/SF_6 Protective Atmosphere,* Proceedings of 34th Annual Meeting of IMA, Columbus, Ohio, 1977,pp 16-20.
7. H. R. Griem and R. H. Lovberg, *Plasma Physics, Academic Press, Science,* 1970, vol **9**, p.p. 201.
8. C. Makochekanwa, M. Kimura and O. Sueoka, *Phys. Rev. A,* 2004, **70**, 022702.
9. M. S. Dababneh, *Phys. Rev. A,* 1988, **38**, 1207.
10. R. E. Kennerlya, R. A. Bonhamb and M. McMillanc, *J. Chem. Phys.,* 1979, **70**, 2039.
11. G. Kasperski, M. Mozejko and C. Szmytkowski, *Z. Phys. D: At., Mol. Clusters,* 1997, **42**, 187.
12. A. Zecca, G. Karwasz and R.S. Brusa, *Chem. Phys. Lett.,* 1992, **199**, 423.
13. H.-X. Wan, J. H. Moore, J. K. Olthoff and R. J. Van Brunt, *Plasma Chemistry and Plasma Processing,* 1993, **19**, 1.
14. J. Ferch, W Raith and K Schroder, *J. Phys. B: At. Mol. Phys.,* 1982, **15**, L175.
15. S. Trajmar, D.F. Register and A. Chutjian, *Physics Reports (Review Section of Physics Letters),* 1983, **97**, 219.
16. P. Limão-Vieira, F. Blanco, J. C. Oller, A. Muñoz, J. M. Pérez, M. Vinodkumar, G. García and N. J. Mason, *Physical Review A,* 2005,**71**, 032720.
17. K. Rohr, *J. Phys. B: Atom. Molec. Phys.,* 1979, **12**, L185.
18. H. Cho, R. J. Gulley, K.W. Trantham, L. J. Uhlmann, C. J. Dedman and S. J. Buckman, *J. Phys. B: At. Mol. Opt. Phys.,* 2000, **33,** 3531.
19. S. K. Srivastava, S. Trajmar, A. Chutjian and W. Williams, *J. Chem. Phys.,* 1976, **64**, 2767.
20. W. M. Johnstone and W. R. Newell, *J. Phys. B: At. Mol. Opt. Phys.*1991, **24**, 473.
21. T. Sakae, S. Sumiyoshi, E. Murakami, Y. Matsumoto, K. Ishibashi and A. Katase, *J. Phys. B: At. Mol. Opt. Phys.,* 1989, **22**, 1385.
22. M. G Benedict and I. Gyemant, *International Journal of Quantum Chemistry,* 1978, **13**, 597.
23. A. V. Phelps and R. J. Van Brunt, *J. Appl. Phys.,* 1988, **64**, 4269.
24. L. G. Christophorou and J. K. Olthoff, *J. of Phys Chem Ref. Data,* 2000, **29**, 267.
25. C. Winstead and V. McKoy, *J. Chem. Phys.,* 2004, **121**, 5828.
26. J. L. Dehmer, Jon Siegel and Dan Dill, *J. Chem. Phys.,* 1978, **69**, 5205.
27. F. A. Gianturco, R. R. Lucchese and N. Sanna, *J. Chem. Phys.,* 1995, **102**, 5743.
28. F. A. Gianturco and R. R. Lucchese, *J. Chem. Phys.,* 2001, **114**, 3429.
29. Y. Jiang, J. Sun and L. Wan, *Phy. Rev. A,* 1995, **52**, 398.
30. W. M. Johnstone and W. R. Newell, *J. Phys. B: At. Mol. Phys.,* 1991, **24**, 473.
31. D.H. Shi, J.F. Sun, Y.F. Liu, Z.L. Zhu and H. Ma, *Eur. Phys. J. D,* 2009, **54**, 43.
32. M. Vinodkumar, K.N. Joshipura and N.J. Mason, *acta physica slovaca,* 2006, **56**, 521.
33. K. N. Joshipura, M. Vinodkumar, C. G. Limbachiya and B. K. Antony, *Physical Review A,* 2004, **69**, 022705.
34. I.I. Fabrikant, H. Hotop and M. Allan, *Physical Review A,* 2005, **71**, 022712.
35. J. M. Carr, P. G. Galiatsatos, J. D. Gorfinkiel, A. G. Harvey, M. A. Lysaght, D. Madden, Z. Mašín, M. Plummer, J. Tennyson and H.N. Varambhia, *Euro. J. Phys. D,* 2012, **66**, 58.
36. J. Tennyson, D. B. Brown, J. M. Munro, I. Rozum, H. N. Varambhia and N. Vinci, *J. Phys. Conf. Ser.,* 2007, **86**, 012001.
37. A. Jain, *J. Chem. Phys.,* 1987, **86**, 1289.
38. B. Goswami, R. Naghma and B. Antony, *Physical Review A,* 2013, **88**, 032707.
39. M. Vinodkumar, A. Barot and B. Antony, *J. Chem. Phys.,* 2012, **136**, 184308.
40. D. Gupta, R. Naghma, B. Goswami and B. Antony, *RSC Adv.,* 2014, **4**, 9197.
41. CCCBDB at http://cccbdb.nist.gov.
42. J. Tennyson, *Phys. Rep.,* 2010, **491**, 29.
43. C.W. Patterson, F. Herlemont, M. Azizi and J. Lemaire, *J. Mol. Spect.,* 1984, **108**, 31.
44. J. Troe, T. M. Miller and A. A. Viggiano, *J. Chem. Phys.,* 2012, **136**, 121102.
45. D. Kajiya and K. Saitow, *J. Phys. Chem. B,* 2010, **114**, 8659.
46. Z. L. Wang, *Philosophical Magazine B,* 1998, **77**, 787.
47. S. N. Altunata, S. L. Coy, and R. W. Field, *J. Chem. Phys.,* 2005, **123**, 084318.
48. B. M. Wong, S. N. Altunata, and R. W. Field, *J. Chem. Phys.,* 2006, **124**, 014106.
49. A. M. Arthurs and A. Dalgarno, *Proc. Phys. Soc. Lond. A,* 1960, **256**, 540.
50. A. Faure, J. D. Gorfinkiel, L. A. Morgan and J. Tennyson, *Comput. Phys. Commun.,* 2002, **144**, 224.
51. M. Gailitis, *J. Phys. B,* 1976, **9**, 843.
52. S. I. Chu and A. Dalgarno, *Phys. Rev. A,* 1974, **10**, 788.
53. N. Sanna and F. A. Gianturco, *Comput. Phys. Commun.,* 1998, **114**, 142.
54. F. Salvat, J. D. Martinez, R. Mayol and J. Parellada, *Physical Review A,* 1987, **36**, 467.
55. S. Hara, *J. Phys. Soc. Jpn.,* 1967, **2**, 710.
56. X. Zhang, J. Sun and Y. Liu, *J. Phys. B: At. Mol. Phys.,* 1992, **25**, 1893.
57. G. Staszewska, D.W. Schewenke, D. Thirumalai and D.G. Truhlar, *Phys. Rev. A,* 1983, **28**, 2740.
58. C. J. Joachain, 1983, *"Quantum Collision Theory"* (Amsterd am: North-Holland).
59. S. Trajmar and A. Chutjian, *J. Phys. B: At. Mol. Phys.,* 1977, **10**, 2943.
60. D. Field, N. C. Jones and J.-P. Ziesel, *Physical Review A,* 2004, **69**, 052716.